

Accepted Manuscript

Removing rubidium using potassium cobalt hexacyanoferrate in the membrane adsorption hybrid system

T. Nur, P. Loganathan, M.A.H. Johir, J. Kandasamy, S. Vigneswaran

PII: S1383-5866(17)31380-1
DOI: <https://doi.org/10.1016/j.seppur.2017.09.048>
Reference: SEPPUR 14057

To appear in: *Separation and Purification Technology*

Received Date: 4 May 2017
Revised Date: 22 September 2017
Accepted Date: 22 September 2017

Please cite this article as: T. Nur, P. Loganathan, M.A.H. Johir, J. Kandasamy, S. Vigneswaran, Removing rubidium using potassium cobalt hexacyanoferrate in the membrane adsorption hybrid system, *Separation and Purification Technology* (2017), doi: <https://doi.org/10.1016/j.seppur.2017.09.048>

This is a PDF file of an unedited manuscript that has been accepted for publication. As a service to our customers we are providing this early version of the manuscript. The manuscript will undergo copyediting, typesetting, and review of the resulting proof before it is published in its final form. Please note that during the production process errors may be discovered which could affect the content, and all legal disclaimers that apply to the journal pertain.



Removing rubidium using potassium cobalt hexacyanoferrate in the membrane adsorption hybrid system

T. Nur, P. Loganathan, M.A.H. Johir, J. Kandasamy, S. Vigneswaran

Faculty of Engineering, University of Technology Sydney (UTS), P.O. Box 123, Broadway, NSW 2007, Australia

*Corresponding author. Tel.: +61 2 95142641, fax: +61 2 95142633.

Email: s.vigneswaran@uts.edu.au

Abstract

Highly-priced rubidium (Rb) can be effectively extracted from seawater using potassium cobalt hexacyanoferrate (KCoFC) and ammonium molybdophosphate (AMP) adsorbents in the membrane adsorption hybrid system (MAHS). KCoFC (< 0.075 mm), KCoFC (0.075 – 0.15 mm), and AMP (< 0.075 mm) had Langmuir adsorption capacities of 145, 113, and 77 mg/g at pH 6.5-7.5, respectively. When KCoFC (< 0.075 mm) at a dose of 0.2 g/L was initially added to 4 L of a solution containing 5 mg Rb/L in the MAHS and 25% of the initial dose was repeatedly added every hour, the amount of Rb removed remained steady at 90-96% for the experiment's 26 h duration. The removal of Rb by AMP under similar conditions was 80-82%. The cumulative Rb removed by KCoFC (< 0.075 mm) in MAHS was only 33% reduced in the presence of high concentrations of other cations in synthetic seawater compared to that in solution containing only Rb. Approximately 30% of the adsorbed Rb was desorbed using 1 M KCl. When the desorbed solution was passed through a column containing resorcinol formaldehyde (RF), 35% of the Rb in the desorbed solution was adsorbed on RF. Furthermore 50% of the Rb adsorbed on RF was recovered by 1 M HCl leaching of the column. This sequence of concentration and separation of Rb in the

presence of other cations in synthetic seawater is an efficient method for recovering pure Rb from real seawater and seawater reverse osmosis brine.

Keywords: rubidium, potassium cobalt hexacyanoferrate, ammonium molybdophosphate, membrane-adsorption hybrid system, seawater.

1. Introduction

Rubidium (Rb) is one of the world's most highly priced alkali metals and it has a range of uses, such as glass types for electrical conductivity, fibre optic and telecommunication systems and night-vision equipment [1,2]. It also has applications in soporifics, sedatives and the treatment of epilepsy and optical application with the usage of warm Rb vapour [3,4]. Because of its high price and numerous uses, Rb extraction from solutions can be very cost-effective [5]. Sea water and sea water rejected brine are good sources of Rb, but its recovery from these sources is challenging due to: firstly, its low concentration; and secondly, limited selectivity of chemicals utilised for its extraction in the presence of high concentrations of other ions in sea water and the brines [6]. The methods currently employed for extracting Rb consist of ion exchange/adsorption, evaporation, precipitation, use of emulsion membranes and liquid–liquid extraction techniques [7,8]. Of these, the ion exchange/adsorption process is the most suitable and widely utilised, since it is able to selectively extract low concentrations of Rb from mixed solutions [9–11].

A wide range of adsorbents such as clay materials [12], prussian blue [13], potassium metal hexacyanoferrate [6,14], zeolite [15], titanosilicate [16] and ammonium molybdophosphate [17] have been used to selectively remove alkali metals. Most of these studies were conducted in batch experiments, and only a few had been reported in fixed-bed

column system studies [18]. Of the various adsorbents, potassium cobalt hexacyanoferrate (KCoFC) and ammonium molybdophosphate (AMP) have indicated high adsorption capacity and selectivity for Rb and cesium (Cs) extraction in both batch and column studies [10,11,17]. Since AMP and KCoFC are of small size (0.075-0.45 mm), they can cause practical problems in column operations due to high-pressure development and the pores becoming clogged. These problems can be overcome by either encapsulating the material in a coarser material or physically mixing it with a coarser material such as granular activated carbon [11,19].

The MAHS is a combination of adsorption and membrane filtration of the adsorbent that can be easily regenerated and reused in the process. Interest in this hybrid process of removing organic and inorganic materials has recently increased because of the continuous removal process with new addition or replacement of adsorbent when the initially added adsorbent is exhausted, which leads to the process costing less [20,21]. Moreover, it has various advantages such as the process is dynamic with treatment employing a large quantity of water, controllable membrane fouling, low capital and operational costs, and considerably less energy requirements [20,21].

The main advantage of the MAHS in comparison to the traditional fixed-bed column adsorption in real water/wastewater treatment plant is that very small sized adsorbent particles can be employed in MAHS. This cannot be done in column experiments because the small particles reduce the flow rate and more energy is needed to pump the feed water [22]. Smaller sized particles can increase the interface area and result in higher adsorption capacity. In MAHS the particles are kept in suspension by pumping air into the system, and this reduces membrane fouling via the scouring effect of adsorbents on the membranes [23,24]. Studies using MAHS have reported the removal of organic micropollutants [25], boron [26], phosphate [27], nitrate [28], colour and reactive dyes [29]. However, no analysis has yet reported the removal of alkali metals such as Rb using MAHS.

The objectives of this research were to: (i) evaluate the performance of KCoFC and AMP for Rb adsorption in batch and MAHS methods; (ii) investigate the effect of adsorbent dose and particle size and water flux on Rb adsorption in the MAHS system; (iii) evaluate the effect of co-existing ions in seawater on Rb adsorption by KCoFC in the MAHS method; and (iv) investigate the efficiency of recovery of Rb by desorption of Rb previously adsorbed on KCoFC in the MAHS experiment followed by its purification using resorcinol formaldehyde (RF) ion exchange resin.

2. Material and methods

2.1. Adsorbent

2.1.1. Potassium hexacyanoferrate (KCoFC)

A commercially available adsorbent, KCoFC (also known as CsTreat) acquired from Fortum Engineering Ltd, Finland was used as the primary adsorbent in this study. This granular adsorbent was dark brown-black in colour and size ranged from 0.25 to 0.85 mm [30]. It has a surface area of 72.1 m²/g, total pore volume of 0.37 cm³/g and pore diameter of 20.5 nm which indicate the adsorbent consists mainly of mesopores (2–50 nm). These and other characteristics of the adsorbent are reported in our previous research [10]. In our previous studies, KCoFC with a 0.15-0.25 mm particle size range was used. In order to increase the adsorption capacity a smaller particle size range of < 0.075 mm to 0.15 mm was utilised in this study.

2.1.2. Ammonium molybdophosphate (AMP)

AMP, which consists of the inorganic salt of phosphomolybdic acid with the chemical formula of (NH₄)₃PMo₁₂O₄₀ was also used as an adsorbent in the study. It was obtained in powder form (< 0.075 mm) from Sigma-Aldrich (Australia). It is a phosphomolybdate ion complex previously used for Cs removal [17].

2.2. Zeta potential analysis

Zeta potential is the electrical potential close to a particle surface where adsorption of ions from the solution phase occurs, and it is positively related to the surface charge. It is an important parameter used for understanding the mechanism of adsorption. The zeta potential values were measured separately on 0.05 g/L of KCoFC and AMP suspensions in solutions of DI water and 10^{-3} M RbCl in the pH range of 2.5-10.0 using a Zetasizer Nano instrument (Nano ZS Zen3600, Malvern, UK). Triplicate measurements were made to minimise undesirable biases (with differences between replicates always been less than 5%), and the average value was used for data analyses.

2.3. Feed solutions and chemical analysis

Feed solutions of different concentrations were prepared using analar grade chemicals – RbCl, KCl, NaCl, CaCl_2 and MgCl_2 (Sigma-Aldrich). Rb, K, Na, Ca, and Mg concentrations were determined using Microwave Plasma - Atomic Emission Spectroscopy (MP-AES) (Agilent 4100).

2.4. Batch adsorption experiment

2.4.1. Effect of pH on Rb adsorption

The influence of pH on Rb adsorption was studied by adding 0.05 g of KCoFC or AMP to 100 mL solutions containing 5 mg Rb/L, and the suspensions were agitated in a flat shaker at a shaking speed of 120 rpm at room temperature (24 ± 1 °C) for 24 h. The solutions' pH levels were initially set at different values within a range of 2.5 – 10.0 using 0.1 M HCl and

0.1 M NaOH. Because the pHs changed during the adsorption process, they were adjusted back to their initial values after 4 h and the shaking of the suspensions continued. The final pHs at the end of the shaking period were measured. A HQ40d portable pH Meter was used for all pH measurements.

2.4.2. Adsorption equilibrium

Equilibrium adsorption experiments were conducted with KCoFC and AMP at adsorbent doses of 0.03 - 1.0 g/L in a set of glass flasks with 100 mL solutions spiked with Rb at a concentration of 5 mg/L and pH 6.5 - 8.0. This concentration of Rb was selected to achieve a close match with the low concentrations of Rb in seawater and to consistently measure the metal concentration using standard analytical instruments. The suspensions were shaken in a flat shaker with a shaking speed of 120 rpm at room temperature (24 ± 1 °C) for 24 h. The amount of Rb adsorbed at equilibrium, q_e (mg/g), was calculated using Eq. (1).

$$q_e = \frac{(C_0 - C_e)V}{M} \quad (1)$$

where C_0 = initial concentration of Rb (mg/L); C_e = equilibrium concentration of Rb (mg/L); V = volume of the solution (L); and M = mass of adsorbent (g). The adsorption data were fitted to the Langmuir adsorption model described elsewhere [10].

2.4.3. Adsorption kinetics

Batch adsorption kinetic experiments were conducted with a fixed dose of 0.2 g/L of KCoFC and AMP with the Rb feed solution concentration of 5 mg/L. The flasks were agitated in a flat shaker at a shaking speed of 120 rpm at room temperature (24 ± 1 ° C) and samples

were taken at different time intervals. The concentrations of Rb in the samples were measured and the amount of Rb adsorption at time t , q_t (mg/g) was calculated using Eq. (2).

$$q_t = \frac{(C_0 - C_t)V}{M} \quad (2)$$

where C_0 = initial concentration of Rb (mg/L); C_t = concentration of Rb at time t (mg/L); V = volume of the solution (L) and M = mass of dry adsorbent used (g).

2.5. Membrane adsorption hybrid system (MAHS)

A schematic diagram of MAHS is shown in Fig. 1 where a hollow fibre microfilter membrane was submerged in a reactor tank of 6 L capacity which was filled with 4 L feed water. The hollow fibre membrane had the specifications of 0.1 μm nominal pore size and 0.1 m^2 surface area. It consisted of hydrophilic modified polyacrylic nitrile (PAN) with 1.1 mm inner and 2.1 mm outer diameters and was obtained from Mann + Hummel, Singapore. The membrane module was positioned in the centre of the reactor tank. Air bubbles were continuously passed at a fixed rate of 1.8 m^3/m^2 membrane area from the bottom of the tank which was predetermined and could sufficiently keep the adsorbent particles in suspension. A peristaltic pump served to withdraw the effluent and to feed new synthetic water at a controlled flux. Two flux rates (10 and 20 $\text{L}/\text{m}^2\text{h}$) were utilised in these experiments to examine the adsorbents' dynamic adsorption performance. The effluent samples were collected at predetermined time intervals for analysis.

KCoFC and AMP doses of 0.05, 0.1 and 2.0 g/L of the reactor volume were used in the experiments with an initial Rb concentration of 5 mg/L. Each adsorbent was added to the tank only once, at the initial stage of the experiment. In subsequent experiments, 25% of initial doses of adsorbent were repeatedly added at every hour continuously for providing new sites

for Rb adsorption. After each experiment, chemical cleaning of the membrane was done using 5% NaOH solution. In this cleaning procedure, the membrane was placed inside the NaOH solution and shaken for 3 h. The membrane was then cleaned with 0.5% NaOCl solution for another 3 h. After cleaning the membrane, filtration flux was checked by filtering distilled water and comparing its flux with that of a virgin membrane. The fluxes were found to be almost similar with a slight variation of around $\pm 5\%$. Only KCoFC was used in the subsequent experiments because of its higher Rb adsorption capacity than AMP.

To inspect the Rb adsorption behaviour of the KCoFC in MAHS system in real seawater conditions, an experiment was conducted on Rb adsorption from synthetic seawater containing Na, Mg, Ca, K, and Rb concentrations (g/L) of 20, 2, 1, 0.85, and 0.005, respectively. An initial dose of KCoFC of 0.2 g/L and addition of 25% of initial doses of adsorbent every hour was used in this experiment.

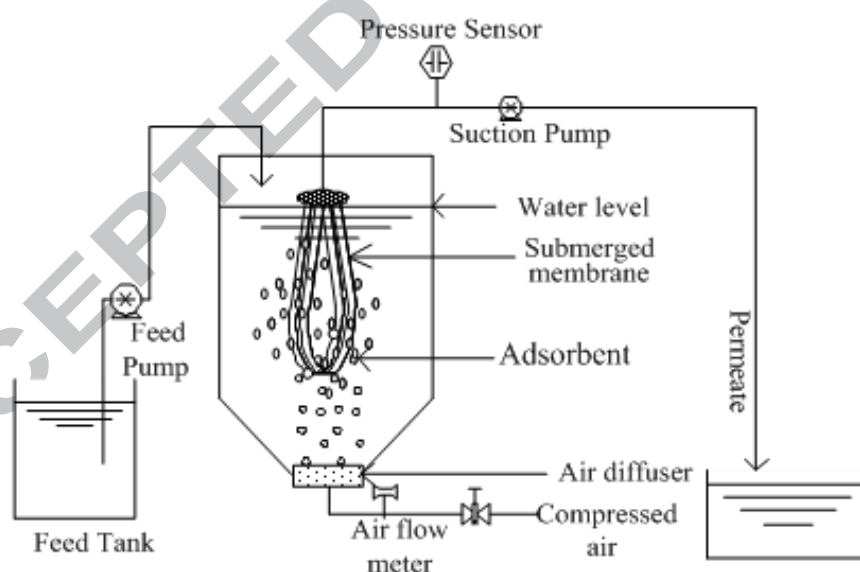


Fig. 1. Schematic diagram of the MAHS

2.6. Desorption

At the end of all the adsorption experiments with both adsorbents in MAHS, the used adsorbent was collected from the reactor by filtering the suspensions. The residues were combined, washed with MQ water, and dried at room temperature ($24 \pm 1^\circ \text{C}$) for 24 h. The dried adsorbent was weighed, and duplicate subsamples were desorbed with 100 mL of 0.1 M and 0.5 M KCl and NH_4Cl in a flat shaker at a shaking speed of 150 rpm for 3 h [10,11].

2.7. Rb recovery using RF resin

Resorcinol formaldehyde (RF) resin was employed in this study for the recovery and purification of Rb that was desorbed from KCoFC after the adsorption experiment with synthetic seawater solution. RF resin is a useful phenolic resin which is formed by the polycondensation of resorcinol and formaldehyde in alkaline solution and used to remove Cs from radioactive solutions [31,32]. RF resin was prepared by mixing resorcinol, formaldehyde, NaOH and H_2O at a molar ratio of 1:2.5:1.5:50 according to the procedure utilised by Samanta et al. [31]. The dark-red coloured mixed solution was then oven dried at 100°C for 24 h, and the dried reddish-brown RF resin product was crushed and sieved to 0.25 - 0.45 mm particle size. The sieved RF resin was then washed with 1 M HCl to convert RF resin to an acid form (H^+) followed by washing it thoroughly with MQ water to convert it to a neutral form and dried at room temperature ($24 \pm 1^\circ \text{C}$) for 24 h. The H^+ form of the resin was then conditioned with 1 M KOH by shaking 5 g of the resin in 500 mL solution at 150 rpm for 24 h to convert it to a K^+ form [33]. Earlier studies have shown that the weakly acidic phenolic $-\text{OH}$ functional groups of the resin responsible for ion exchange were expected to fully realise their ion-exchange properties only if the $-\text{OH}$ groups were ionised to the highest extent which occurs in alkaline solutions such as KOH [31,34]. The K^+ form of the resin was

thoroughly washed with MQ water to remove excess KOH, dried at room temperature ($24 \pm 1^\circ\text{C}$) for 24 h and kept stored in an air-tight container.

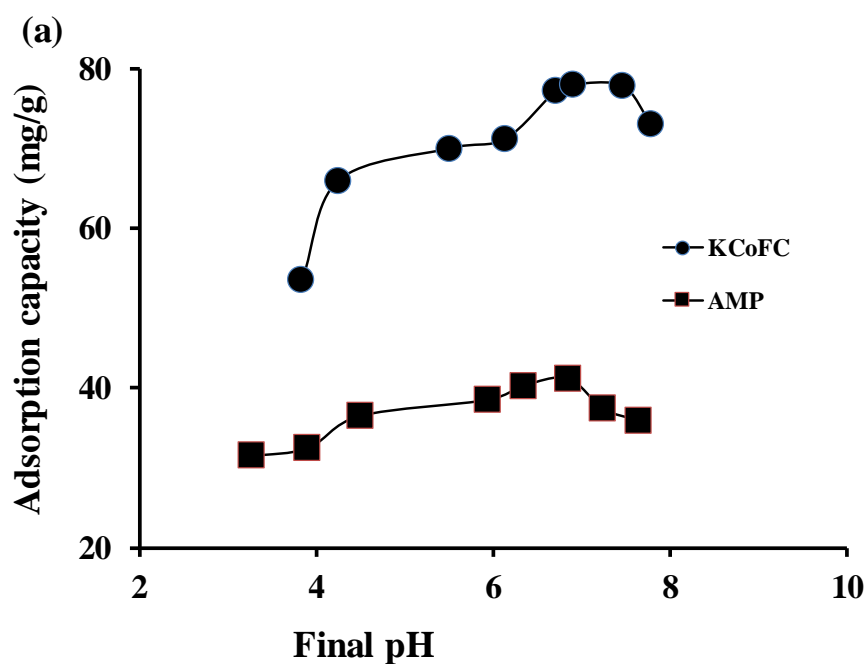
The desorbed solution obtained by KCl leaching of the KCoFC column after the adsorption experiment with synthetic seawater solution was used in the Rb recovery experiment. This solution was passed upward through a pyrex glass column (1.8 cm inner diameter) packed with 10 g RF resin to a height of 6 cm at a filtration velocity of 2.5 m/h. The progress of Rb loading was monitored by periodic measurement of Rb in the effluent samples to ensure that maximum amount of Rb in the desorbed solution was adsorbed to RF. The adsorbed Rb was eluted from the resin with 0.1 M HCl for about 40 h followed by further elution with 1.0 M HCl for 10 h, both elutions were at a flow rate of 5 m/h. 0.1 M HCl was used to desorb all cations other than Rb (Na, Ca, Mg and K) which were weakly adsorbed to RF. The subsequently used higher concentration of HCl was to desorb the strongly adsorbed Rb [33].

3. Results and discussion

3.1. Effect of pH on Rb adsorption

The adsorption capacity of KCoFC and AMP in the pH 2.5-10 range revealed that the adsorption capacity increased when pH also rose (Fig. 2a) and KCoFC and AMP had the highest adsorption capacity at pH 7.0 - 7.5 and 6.5 - 7.0, respectively. The increase in adsorption is inversely related to their zeta potentials (Fig. 2b). Zeta potential of KCoFC and AMP decreased from -0.5 to -24 mV as the pH increased from 3.0 to 8.0. The number of negative charges on the surface of the adsorbent increased with pH. Therefore, the increase in pH elevated the adsorption of positively charged Rb ions by electrostatic adsorption (outer-sphere complexation) [10,11]. Moreover, at low pH, H^+ could have competed with Rb for

adsorption in the highly acidic solution where the concentration of H^+ was high, and consequently adsorption capacity declined. Similarly, at high pH the presence of increased concentration of Na (arising from pH adjustment with NaOH) most likely competed with Rb adsorption, thus reducing Rb adsorption capacity [10,11]. The results also indicated that the difference between the zeta potential with and without Rb increased, and the negative surface charge declined in the presence of Rb as pH increased for both adsorbents (Fig. 2b). This meant that Rb was also absorbed by the inner-sphere complexation mechanism [35]. Based on these results, all the remaining experiments were done at pH 6.5 - 7.0 for AMP and at pH 7.0 - 7.5 for KCoFC, the pHs at which the highest adsorption capacities were obtained.



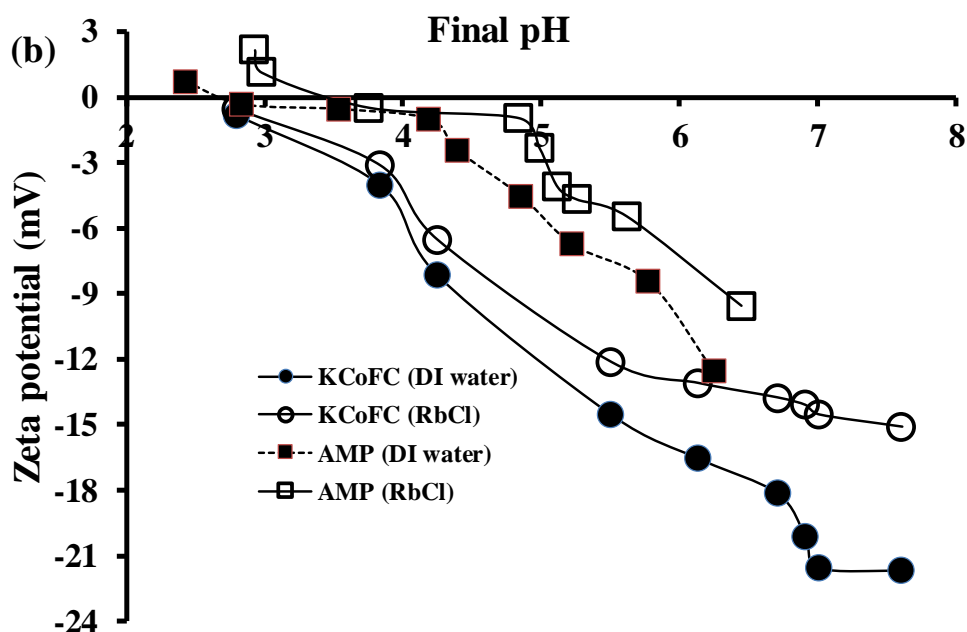


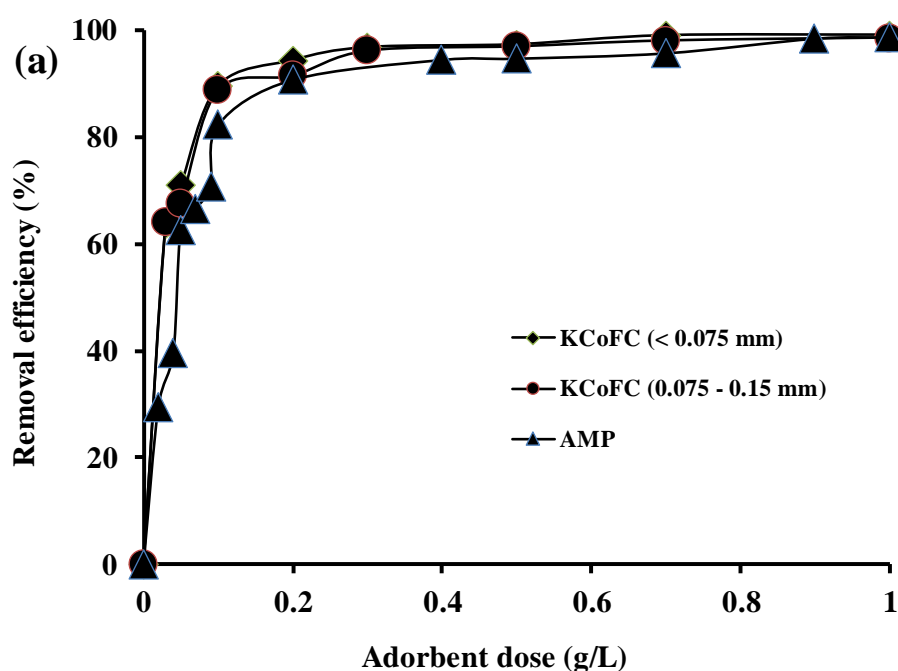
Fig. 2. Effect of (a) pH on Rb adsorption by KCoFC and AMP and (b) zeta potential trend as a function of pH in the presence of RbCl (10^{-3} M) and DI water (adsorbent dose 0.05 g/L).

3.2. Batch equilibrium experiment

The results of the equilibrium experiments with two particle sizes of KCoFC (< 0.075 mm and 0.075 - 0.15 mm) and AMP (< 0.075 mm) revealed that the KCoFC had a higher Rb removal efficiency (92 - 94%) for both particle sizes than AMP (90%) at the dose of 0.2 g/L and initial Rb concentration of 5 mg/L (Fig. 3a). The adsorption isotherm data satisfactorily fitted to the Langmuir adsorption model ($R^2 = 0.96 - 0.98$) (Fig. 3b) for both adsorbents. The maximum adsorption capacities calculated from the model were 145 and 113 mg /g for the particle sizes of < 0.075 mm and 0.075 - 0.15 mm of KCoFC, respectively, and 77 mg/g for AMP. The adsorption capacity of AMP was higher than the value of 51 mg/g in a previous study on AMP [19]. The adsorption capacities of KCoFC were also higher than the value of

96 mg/g [10] reported in our previous research on KCoFC with particle size of 0.25 - 0.45 mm. This is because smaller particle sizes used in the present study had higher surface area to absorb more Rb than the larger size particles used in our earlier study. The adsorption capacity of KCoFC (< 0.075 mm) is higher than almost all adsorbents reported in literature including nanomaterials (Table 1). The higher adsorption capacity of KCoFC is due to the exchange of structural K by Rb [10]. Furthermore, the selectivity of Rb adsorption in the presence of other ions in seawater was very high. Most of the other adsorbents, for example graphene has higher selectivity towards Li, Na, and K adsorption and not for Rb [44]

KCoFC had a higher adsorption capacity than AMP, which is consistent with the zeta potential results that KCoFC had higher negative zeta potential values than AMP (Fig. 2b). Moreover, the amount of theoretically interchangeable K ions in the KCoFC structure is close to 3.3 mmol/g [10] while the amount of potentially exchangeable ammonium (NH_4) ions in AMP is about 1.6 mmol/g [19]. This means that KCoFC had about three times more exchangeable reactive groups than AMP and thus exhibited higher adsorption capacity.



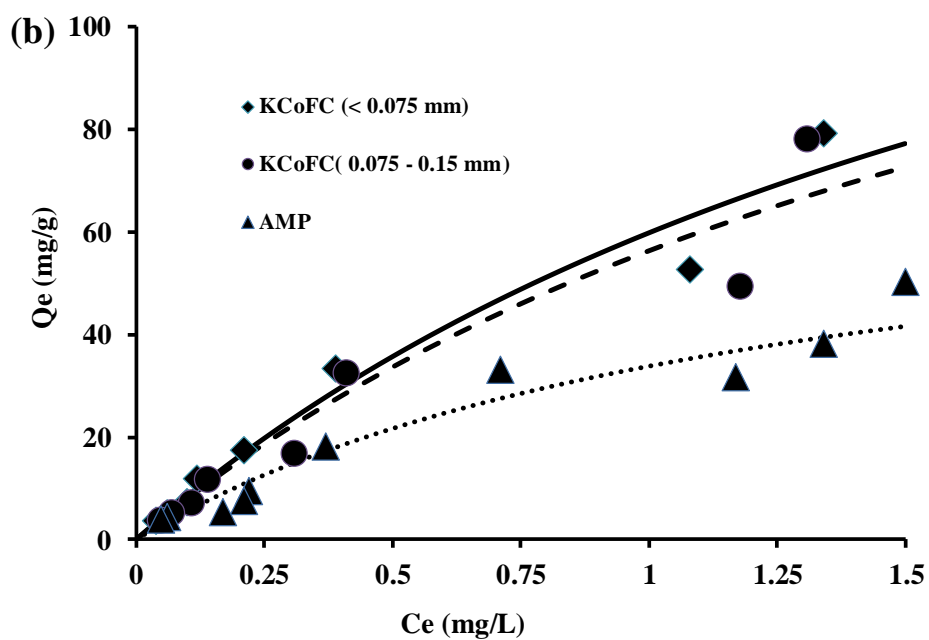


Fig. 3. Effect of (a) adsorbent dose on Rb removal efficiency (initial concentration of Rb was 5 mg/L) and (b) Langmuir model plot for the data (Q_e , amount of Rb adsorbed; C_e , equilibrium solution concentration of Rb) on Rb adsorption on KCoFC and AMP [KCoFC < 0.075 mm (—), 0.075 - 0.15 mm (- -), AMP (···)].

Table 1.

Comparison of Langmuir adsorption capacity for Rb on KCoFC with that on other adsorbents.

Adsorbent	Experimental conditions	Adsorption capacity (mg/g)	Reference
Modified polyaniline nanocomposite (PANI/Co-PBA/NC)	pH 5.0; 25°C	98.0	[36]
Ion-imprinted polymeric nanoparticles	pH 9.0; 25°C	5.4	[37]
Thiacalixarene-functionalized Graphene Oxide	pH 7.0; 25°C	164.5	[38]
Nanofibrous manganese Oxide	-	87.6 (ion exchange capacity)	[39]
Potassium hexacyanoferrate (CsTreat)	pH 7.8; 21°C	46.7	[6]
Potassium iron(III) hexacyanoferrate polymethylmethacrylate	pH 7.0; 25°C	79.9	[40]
Ammonium molybdophosphate (AMP)	pH 3.0; 25°C	56.1	[19]
Ammonium molybdophosphate-calcium alginate	pH 3.5.0; 25°C	49.6	[41]
Zirconium phosphate (Phozir)	pH 3.0; 25°C	61.1	[19]
Ammonium molybdophosphate + Phozir	pH 3.0; 25°C	62.8	[19]
Imogolite aluminosilicate modified mercaptothiazoline (IMOMTZ)	pH 4.0; 25°C	26.1	[42]
Chromium terephthalate (MIL-101Cr)/phenol	pH 4.0; 25°C	92.9	[43]
Potassium cobalt hexacyanoferrate (KCoFC)	pH 7.5; 25°C	145	This study
AMP	pH 7.5; 25°C	77	This study

3.3. Batch kinetic experiment

To investigate the adsorption behaviour of the adsorbents with time, a KCoFC and AMP dose of 0.2 g/L was chosen for the kinetic experiments. Results showed that the removal efficiency was 80% and 70% for KCoFC doses of < 0.075 mm and 0.075 - 0.15 mm at 30 min, respectively, and it reached a plateau within 1 h with removal efficiencies of 95% and 93%, respectively (Fig. S1). Rb removal efficiency by AMP also reached the plateau in 1 h with a removal efficiency of 90%. These kinetic experiments showed that both these adsorbents reached adsorption equilibrium within a short period. This information was used in determining the time at which additions of fresh adsorbents are required in the MAHS experiment.

3.4. Membrane adsorption hybrid system (MAHS)

Based on the batch kinetic results, short-term MAHS experiments with KCoFC (< 0.075 mm) and AMP suspensions were conducted with an initial adsorbent dose of 0.2 g/L of the volume of the reactor. As in the batch kinetic experiments it was found that the removal efficiency of Rb reached a very high value within a short period for both adsorbents. The removal efficiencies were approximately 90% and 93% for KCoFC particle size of < 0.075 mm after 30 min and 1 h, respectively, and 80% and 82% for AMP for these two times, respectively, and it decreased after 1 h for both adsorbents (Fig. 4). However, the removal efficiency of KCoFC with a 0.075 - 0.15 mm particle size was considerably poorer than that of the finer particle size. The removal efficiency was 40% for KCoFC of 0.075 - 0.15 mm particle size for the first 10 min and then started to fall. Moreover, the removal rate of Rb decreased with time as the new feed was continuously added, because the adsorbents were increasingly saturated with Rb. Based on these results, KCoFC particle size of < 0.075 mm and AMP were chosen for a long-term MAHS study where fresh adsorbent was added every

hour to maintain the removal efficiency constant. An experiment without using any adsorbent (blank) was also conducted, and the results showed that there was no Rb adsorption when only the membrane (without adsorbent) was used (Fig. 4).

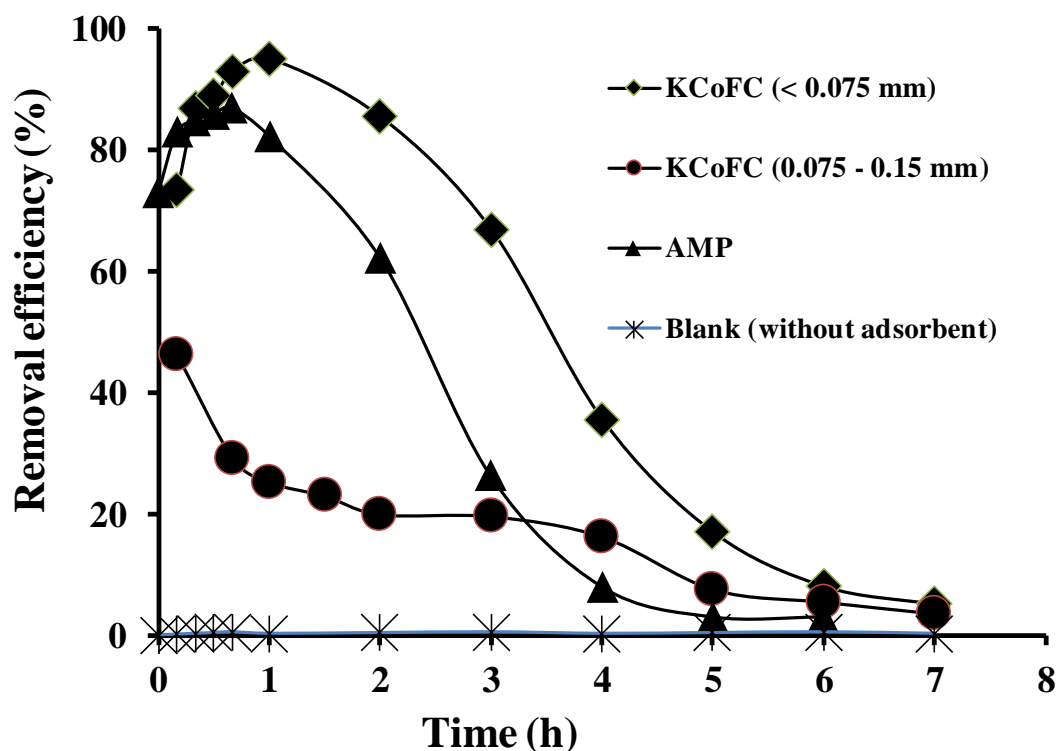


Fig. 4. Effect of time on the removal of Rb by KCoFC and AMP in MAHS (influent Rb concentration = 5 mg/L and adsorbent dose = 0.2 g/L of the volume of the reactor).

3.5. Comparison between KCoFC and AMP

Based on the short-term MAHS results, KCoFC particle size < 0.075 mm and AMP were selected for long-term experiments with adsorbent dose of 0.2 g/L and repeated adsorbents addition of 25% (0.05 g/L) of the initial adsorbent dose at every hour. The removal efficiency remained high and was almost constant due to the frequent fresh additions of adsorbents. The removal efficiency was greater with KCoFC of < 0.075 mm than with AMP.

The removal efficiency for the first 1 h was 95% for KCoFC, and thereafter, it was 93 - 96% up to 26 h of the experiment. On the other hand, the removal efficiency was 82% for the first 1 h and varied from 80 to 82% up to 26 h for AMP (Fig. 5). The total Rb adsorbed was 142 mg (24 mg/g) and 82 mg (14 mg/g) for KCoFC and AMP, respectively

These results imply that: firstly, intermittent addition of the adsorbent helped to maintain continuous removal of Rb; and secondly, KCoFC had higher adsorption capacity than AMP which is consistent with the trend obtained in the batch isotherm study where KCoFC had higher Langmuir adsorption capacity (145 mg/g) than AMP (77 mg/g). However, adsorption capacities in MAHS were much lower than the Langmuir adsorption capacities. The reason for the lower adsorption capacities in MAHS might be the higher mass transfer limitations due to the lower concentration gradient between the solution and the solid surface as well as the shorter contact time between the adsorbate and the adsorbent [28]. On the other hand, the intense agitation in the batch study resulted in longer and closer contacts between the adsorbate and adsorbent and produced higher adsorption capacity. Based on the results of this experiment, KCoFC was chosen for further MAHS experiments to examine the effect of adsorbent dose and solution flux on the removal efficiency of Rb and recovery of Rb from synthetic seawater.

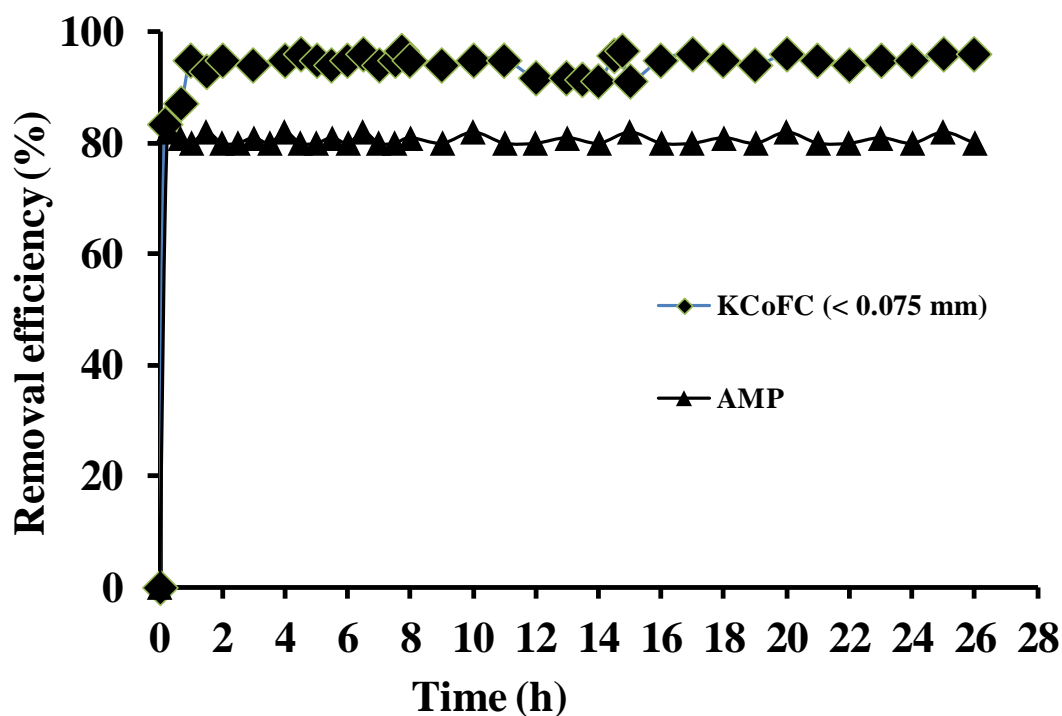


Fig. 5. Comparison of Rb removal efficiencies of KCoFC and AMP in MAHS system with the addition of 25% of the initial dose of adsorbent every hour (inlet concentration of Rb 5 mg/L, flux 10 L/ m²h and adsorbent dose 0.2 g/L of membrane reactor volume).

3.6. Effect of different MAHS parameters on Rb removal

3.6.1. Adsorbent dose

Different doses of KCoFC were studied in the MAHS system to determine the dose which produces the highest Rb adsorption. The influent solution was delivered to the suspension tank at 16.6 mL/min, and adsorbent was added repeatedly at 25% of the initial adsorbent dose at every hour. The Rb removal efficiency was 62 - 73%, 63 - 92% and 93 - 96% for the adsorbent doses of 0.05, 0.1 and 0.2 g/L (Fig. S2). The cumulative amount of Rb adsorption also rose with the increased amount of adsorbent (Fig. 6). A similar phenomenon was also observed in a previous study on the removal of boron from seawater [45] and phosphate from wastewater [27] in continuously operated MAHS. The amounts of Rb

adsorbed during the 26 h of experiments were 90, 124 and 142 mg for the adsorbent doses of 0.05, 0.1 and 0.2 g/L, respectively.

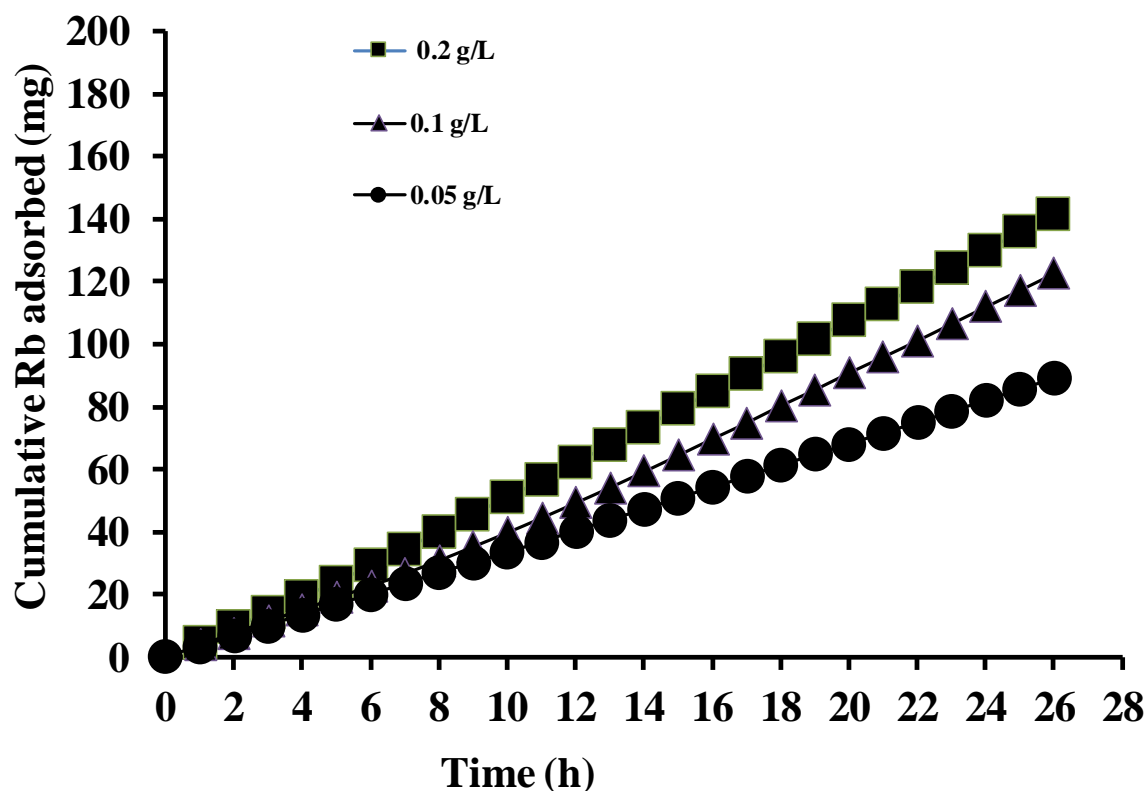


Fig. 6. Effect of initial KCoFC dose with repeated additions of 25% of the doses at every hour on the cumulative Rb adsorbed in MAHS experiment (influent Rb concentration 5 mg/L and flux 10 L/m²h).

3.6.2. Flux

Rb removal at the fluxes of 10 and 20 L/m²h were compared at a KCoFC dose of 0.1 g/L of the volume of the reactor with additions of 25% of the initial adsorbent dose (0.05 g/L) at every hour. The removal efficiency was higher for lower flux than higher flux (Fig. S3) (Table S1), but the total Rb removal was higher at higher flux (Fig. 7). The higher removal efficiency at lower flux could be due to lower hydraulic retention time (HRT). At lower flux

of 10 L/ m²h, the HRT was 4 h, which is almost twice that of 20 L/ m²h. This was because at a filtration rate of 10 L/m²h, the adsorbent was in contact with feed water at twice the rate than at a filtration flux of 20 L/m²h. Thus, it had a considerably longer duration of time to adsorb Rb. However, at the higher flux conditions, KCoFC adsorbed more Rb than at the lower flux because at the higher flux condition, a larger amount of Rb was in contact with the adsorbent per unit time. These trends are the same as those reported for phosphorus removal by zirconium (IV) hydroxide [27] and nitrate removal by different adsorbents [28] at different fluxes in MAHS.

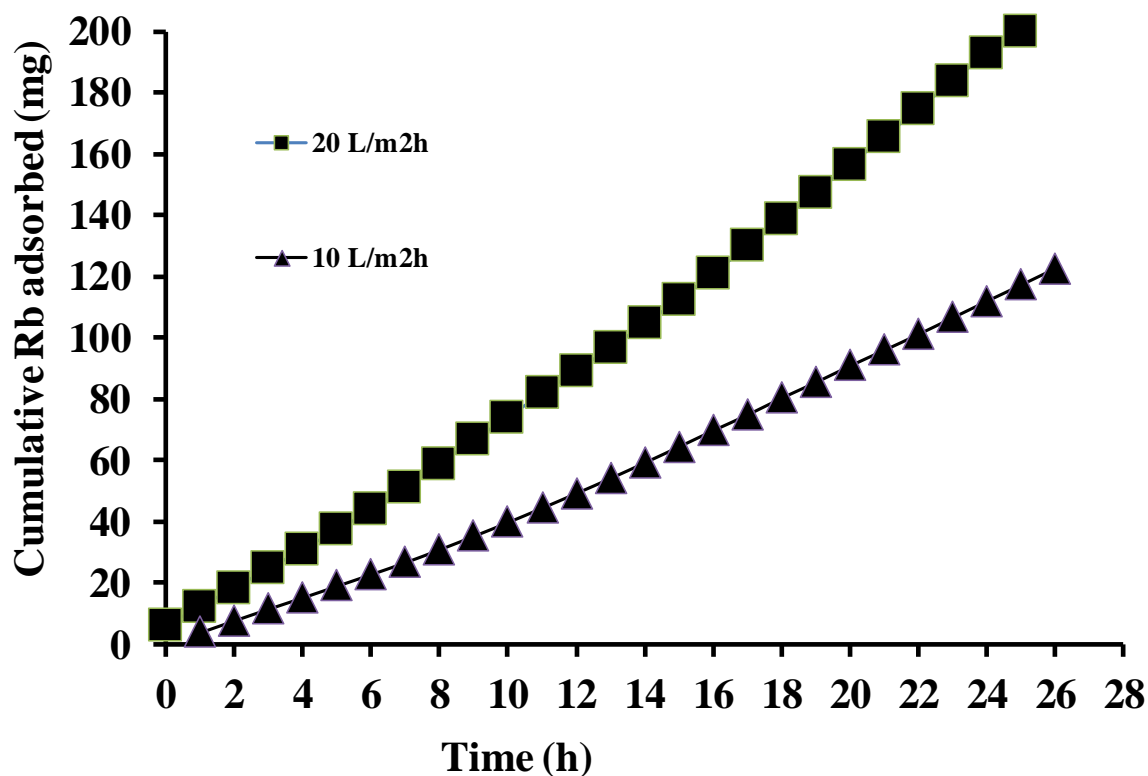


Fig. 7. Effect of flux on cumulative Rb adsorbed by KCoFC with repeated additions of 25% of the doses at every hour in MAHS (inlet concentration of Rb 5 mg/L with adsorbent dose 0.1 g/L of membrane reactor volume).

3.7. Synthetic seawater Rb adsorption

After determining the optimum parameters for Rb removal in MAHS using a solution containing Rb only, the behaviour of KCoFC in removing Rb from synthetic seawater in MAHS was investigated. It emerged that the removal efficiency of Rb (16 mg/g) fell by only 33% from the removal efficiency with Rb only solution (24 mg/g), in the presence of other ions in seawater at much higher concentration than Rb (Fig. S4, Table S1). The cumulative amount of Rb adsorbed was only reduced from 142 mg to 94 mg in 24 h of operation with a

filtration flux of 10 L/m²h and 0.2 g/L adsorbent dose (Fig. 8) (Table S1). These results indicate that KCoFC was selective to the adsorption of Rb and could be successfully used in the recovery of Rb from real seawater.

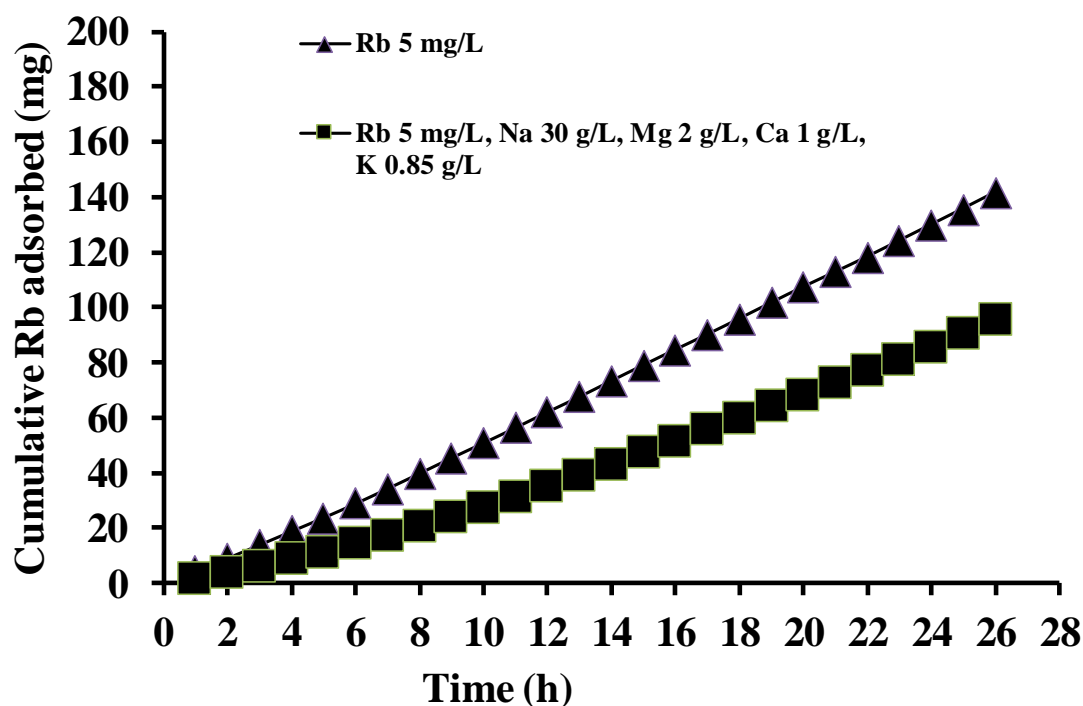


Fig. 8. Effect of seawater co-ions on total Rb adsorbed by KCoFC with repeated additions of 25% of the initial dose at every hour in MAHS (flux of 10 L/ m²h and adsorbent dose of 0.2 g/L of membrane reactor volume).

Rubidium adsorption released Co, Fe and K from the structure of KCoFC into solution. The amount of Co released calculated from our previous study [10] was 0.07 mmol/g of KCoFC in 100 ml solution. Based on this result, for 30 L of Rb solution used in the MAHS, the amount of Co released would be 34 mg. This is equivalent to a Co concentration of 1.1 mg/L. This concentration is higher than the trigger Co concentration limit of 0.05 - 0.1 mg/L for irrigation water and just above the trigger value of drinking water for livestock of 1.0 mg/L [46]. Therefore, the solution left after removing Rb cannot be used for irrigation or drinking water for livestock and need to be disposed back to the sea.

3.9. Desorption

The Rb adsorbed on KCoFC and AMP from Rb only solution was desorbed with 0.1 M and 0.5 M of KCl and 0.5 M NH₄Cl, respectively. It was found that the recovered mass of adsorbent was 95% for KCoFC whereas it was only 72% for AMP (Table 1). This was because of the sticky nature of AMP, which led to the loss of some adsorbent during its collection. KCl was found to be a better desorbing reagent than NH₄Cl for KCoFC as observed in our previous results [10,11]. The desorption capacity was 38% and 90% with 0.1 M and 0.5 M of KCl for KCoFC, respectively. On the other hand, 0.1 M NH₄Cl had only 33% desorption capacity. At the higher concentration (0.5 M), KCl was more efficient than NH₄Cl because K can effectively interchange with adsorbed Rb inside the KCoFC lattice [10]. The situation was the reverse for AMP where NH₄Cl desorbed more Rb than KCl. Previous research has shown that NH₄-based desorbing agents such as NH₄NO₃ successfully eluted Rb from AMP [47]. This is probably due to the preference of NH₄ ion for adsorption on AMP which has a NH₄-based lattice structure [17]. In contrast to the high percentage Rb desorption of 90% obtained with 0.5 M KCl desorbing agent in Rb only solution experiment, the percentage of adsorbed Rb that was desorbed by 1 M KCl in the synthetic seawater experiment was only 30% (Table 2). The much lower percentage of Rb desorbed even using a high concentration of KCl suggests that other seawater ions adsorbed on KCoFC have inhibited the desorption of Rb in the seawater experiment.

Table 2.

Desorption of Rb from KCoFC and AMP using different reagents (desorption was from previously adsorbed Rb on KCoFC at an adsorbent dose of 0.2 g/L with 25% repeated additions every hour; total adsorbent used 5.8 g; experiment duration 26 h)

Adsorbent	Solution type	Total Rb adsorbed (mg)	Recovered adsorbent weight (g)	Recovered weight (%)	Desorbing reagent	Rb desorption capacity (%)
KCoFC < 0.075 mm	Rb	142	4.7	81	0.1 M KCl	38
	5 mg/L				0.5 M KCl	90
					0.1 M NH ₄ Cl	18
					0.5 M NH ₄ Cl	33
					Synthetic seawater	94
AMP < 0.075 mm	Rb	82	3.6	72	0.1 M KCl	6
	5 mg/L				0.5 M KCl	10
					0.1 M NH ₄ Cl	63
					0.5 M NH ₄ Cl	94

3.10. Recovery of Rb using RF resin

A column experiment was conducted using RF resin to recover pure Rb from the desorbed solution obtained by leaching of Rb adsorbed to KCoFC by KCl as conducted in our previous study [33]. The percentage of Rb adsorbed on to the RF column was 35% of Rb in the KCoFC desorbed solution. The low percentage adsorption was due to competition for adsorption from the higher concentrations of other cations. The RF resin was then leached with 0.1 M HCl to remove all cations other than Rb adsorbed on RF, followed by 1 M HCl leaching to desorb the strongly adsorbed Rb that was not significantly removed by the previous leaching with 0.1 M HCl (Fig. 9). Appreciable amounts of Rb were desorbed with 1

M HCl up to 300 bed volumes and then the rate of desorption drastically decreased and reached completion at 800 bed volumes. Approximately 50% of Rb adsorbed on RF resin was desorbed by 1 M HCl. This is equivalent to 17% of Rb desorbed from KCoFC by 1 M KCl and 5% of the 94 mg Rb adsorbed on KCoFC. In a previous study using synthetic solution containing only Rb and K (derived from the desorbing reagent), about 68% of Rb adsorbed on RF resin was recovered [33] compared to the 50% in the present study. The lower percentage obtained in the present study is due to the presence of other coexisting ions in the synthetic seawater. Considering the very high market price of Rb (7857 Euros/kg [6]), even the small recovery of 5% of the Rb adsorbed on KCoFC (3.1% of the Rb in seawater) is economically attractive. This percentage recovery could be increased by increasing the RF dose in MAHS.

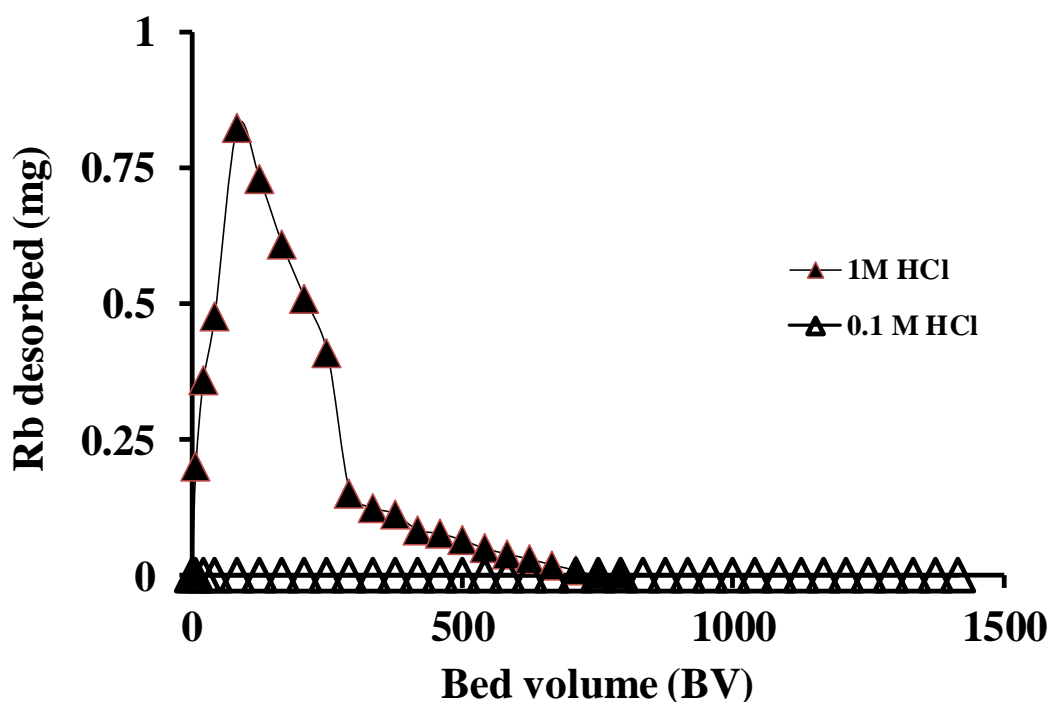


Fig. 9. Rb desorbed from RF resin using 0.1 M HCl and the subsequent desorption by 1 M HCl.

4. Conclusions

KCoFC, which was found to be an attractive adsorbent for the extraction of Rb from synthetic sea water solutions in previous batch and column studies, has proven to be efficient in extracting Rb in MAHS as well. However, unlike in column studies, very fine particle size of KCoFC (< 0.075 mm) which had higher adsorption capacity (145 mg/g) than coarse KCoFC (0.075 – 1.5 mm) (Langmuir adsorption capacity 113 mg/g) could be used in MAHS. Moreover, the adsorbent was added repeatedly to MAHS to maintain the high adsorption capacity over the long-term. The maximum adsorption capacity obtained for KCoFC of particle size < 0.075 mm in the MAHS was 69 mg/g with repeated hourly additions of 25% of the initial dose of 0.2 g/L. This value is higher than the value of 14 mg/g obtained for another efficient Rb adsorbent, specifically AMP. The adsorption capacity of KCoFC (< 0.075 mm) was reduced by only 33% in synthetic seawater containing high concentrations of Na, K, Ca, and Mg compared to Rb-only solution. The desorption of the Rb adsorbed on KCoFC from synthetic seawater solutions using KCl was 30%. The desorbed Rb was adsorbed onto the RF column and subsequently the column was leached first with 0.1 M HCl to remove cations other than Rb and subsequently with 1 M HCl which recovered 50% of the Rb adsorbed to RF. This sequence of concentration and separation of Rb in the presence of other cations is an efficient method for recovering pure Rb from real seawater and seawater reverse osmosis brine.

References

- [1] J. Jandova, P. Dvorák, J. Formánek, H.N. Vu, Recovery of rubidium and potassium alums from lithium-bearing minerals, *Hydrometallurgy* 119 (2012) 73–76.
- [2] W.C. Buttermann, R.G. Reese Jr, Mineral commodity profiles rubidium, U.S. geological survey, Open File Report 03–045 (2003) 3–11.

- [3] F.S. Wagner, Rubidium and Rubidium Compounds, Kirk-Othmer Encyclopedia of Chemical Technology, 2011, pp. 1–11. Available from: <<http://onlinelibrary.wiley.com/doi/10.1002/0471238961.1821020923010714>. a01.pub3> (accessed 10 January 2012).
- [4] M. Hosseini, B.M. Sparkes, G. Campbell, P.K. Lam, B.C. Buchler, High efficiency coherent optical memory with warm rubidium vapour, *Nat. Commun.* 2 (2011) 1–5.
- [5] P. Loganathan, G. Naidu, S. Vigneswaran, Mining valuable minerals from seawater: a critical review, *Environ. Sci.: Water Res. Technol.* 3 (2017) 37–53.
- [6] M. Petersková, C. Valderrama, O. Gibert, J.L. Cortina, Extraction of valuable metal ions (Cs, Rb, Li, U) from reverse osmosis concentrate using selective sorbents, *Desalination* 286 (2012) 316–323.
- [7] B. Mohite, S. Burungale, Separation of rubidium from associated elements by solvent extraction with dibenzo-24-crown-8, *Anal. Lett.* 32 (1999) 173–183.
- [8] M. Shamsipur, K. Alizadeh, M. Hosseini, M.F. Mousavi, M.R. Ganjali, PVC membrane and coated graphite potentiometric sensors based on dibenzo-21-crown-7 for selective determination of rubidium ions, *Anal. Lett.* 38 (2005) 573–588.
- [9] J. Le Dirach, S. Nisan, C. Poletiko, Extraction of strategic materials from the concentrated brine rejected by integrated nuclear desalination systems, *Desalination* 182 (2005) 449–460.
- [10] G. Naidu, T. Nur, P. Loganathan, J. Kandasamy, S. Vigneswaran, Selective sorption of rubidium by potassium cobalt hexacyanoferrate, *Sep. Purif. Technol.* 163 (2016) 238–246.
- [11] T. Nur, G. Naidu, P. Loganathan, J. Kandasamy, S. Vigneswaran, Rubidium recovery using potassium cobalt hexacyanoferrate sorbent, *Desalin. Water Treat.* 57 (2016) 1–9.
- [12] A. Ararem, O. Bouras, F. Arbaoui, Adsorption of cesium from aqueous solution on binary mixture of iron pillared layered montmorillonite and goethite, *Chem. Eng. J.* 172 (2011) 230–236.
- [13] H. Yang, L. Sun, J. Zhai, H. Li, Y. Zhao, H. Yu, In situ controllable synthesis of magnetic Prussian blue/graphene oxide nanocomposites for removal of radioactive cesium in water, *J. Mater. Chem. A* 2 (2014) 326–332.
- [14] J. Moon, E. Lee, H. Kim, Ion exchange of Cs ion in acid solution with potassium cobalt hexacyanoferrate, *Korean J. Chem. Eng.* 21 (2004) 1026–1031.
- [15] A. El-Kamash, Evaluation of zeolite A for the sorptive removal of Cs⁺ and Sr²⁺ ions from aqueous solutions using batch and fixed bed column operations, *J. Hazard. Mater.* 151 (2008) 432–445.
- [16] R. Saberi, A. Nilchi, S.R. Garmarodi, R. Zarghami, Adsorption characteristic of ¹³⁷Cs from aqueous solution using PAN-based sodium titanosilicate composite, *J. Radioanal. Nucl. Chem.* 284 (2010) 461–469.

- [17] Y. Park, Y. Lee, W.S. Shin, S. Choi, Removal of cobalt, strontium and cesium from radioactive laundry wastewater by ammonium molybdophosphate– polyacrylonitrile (AMP–PAN), *Chem. Eng. J.* 162 (2010) 685–695.
- [18] O. Gibert, C. Valderrama, M. Peterková, J.L. Cortina, Evaluation of selective sorbents for the extraction of valuable metal ions (Cs, Rb, Li, U) from reverse osmosis rejected brine, *Solvent Extr. Ion Exch.* 28 (2010) 543–562.
- [19] P. Kryszewski, F. Testa, A. Trochimczuk, C. Pin, J. Taulemesse, T. Vincent, E. Guibal, Encapsulation of ammonium molybdophosphate and zirconium phosphate in alginate matrix for the sorption of rubidium (I), *J. Colloid Interface Sci.* 409 (2013) 141–150.
- [20] N. Kabay, M. Bryjak, S. Schlosser, M. Kitis, S. Avlonitis, Z. Matejka, I. Al-Mutaz, M. Yuksel, M., Adsorption-membrane filtration (AMF) hybrid process for boron removal from seawater: an overview, *Desalination* 223 (2008) 38–48.
- [21] W. Guo, W. Shim, S. Vigneswaran, H. Ngo Effect of operating parameters in a submerged membrane adsorption hybrid system: experiments and mathematical modeling, *J. Membr. Sci.* 247 (2005) 65–74.
- [22] N. Kabay, I. Yilmaz, M. Bryjak, M. Yuksel, Removal of boron from aqueous solutions by a hybrid ion exchange–membrane process, *Desalination* 198 (2006) 74–81.
- [23] M.A.H. Johir, R. Aryal, S. Vigneswaran, J. Kandasamy, A. Grasmick, Influence of supporting media in suspension on membrane fouling reduction in submerged membrane bioreactor (SMBR), *J. Membr. Sci.* 374 (2011) 121–128.
- [24] M.A. Johir, S. Shanmuganathan, S. Vigneswaran, J. Kandasamy, Performance of submerged membrane bioreactor (SMBR) with and without the addition of the different particle sizes of GAC as suspended medium. *Bioresour. Technol.* 141 (2013) 13–18.
- [25] S. Shanmuganathan, T.V. Nguyen, S. Jeong, J. Kandasamy, S. Vigneswaran, Submerged membrane–(GAC) adsorption hybrid system in reverse osmosis concentrate treatment, *Sep. Purif. Technol.* 146 (2015) 8–14.
- [26] M. Bryjak, J. Wolska, N. Kabay, Removal of boron from seawater by adsorption–membrane hybrid process: implementation and challenges, *Desalination* 223 (2008) 57–62.
- [27] M.A.H. Johir, M. Pradhan, P. Loganathan, J. Kandasamy, S. Vigneswaran, Phosphate adsorption from wastewater using zirconium (IV) hydroxide: kinetics, thermodynamics and membrane filtration adsorption hybrid system studies, *J. Environ. Manage.* 167 (2016) 167–174.
- [28] M. Kalaruban, P. Loganathan, J. Kandasamy, S. Vigneswaran, Submerged membrane adsorption hybrid system using four adsorbents to remove nitrate from water, *Sep. Purif. Technol.* (in press).
- [29] J.W. Lee, S.P. Choi, R. Thiruvengatchari, W.G. Shim, H. Moon, Submerged microfiltration membrane coupled with alum coagulation/powdered activated carbon adsorption for complete decolorization of reactive dyes, *Water Res.* 40 (2006) 435–444.

- [30] E. Tusa, R. Harjula, J. Lehto. Use of highly selective ion exchangers for minimization of waste volumes, in: Proceedings of Waste Management Symposium, Tucson, Arizona, USA, 2001.
- [31] S. Samanta, M. Ramaswamy, B. Misra, Studies on cesium uptake by phenolic resins, *Sep. Sci. Technol.* 27 (1992) 255–267.
- [32] C. Dwivedi, A. Kumar, J.K. Ajish, K.K. Singh, M. Kumar, P.K. Watal, P.N. Bajaj, Resorcinol-formaldehyde coated XAD resin beads for removal of cesium ions from radioactive waste: synthesis, sorption and kinetic studies. *RSC Adv.* 2 (2012) 5557–5564.
- [33] G. Naidu, P. Loganathan, S. Jeong, M.A.H. Johir, V.H.P. To, J. Kandasamy, S. Vigneswaran, Rubidium extraction using an organic polymer encapsulated potassium copper hexacyanoferrate sorbent, *Chem. Eng. J.* 306 (2016) 31–42.
- [34] D. Banerjee, R.A. Rao, P.K. Watal, Separation and recovery of Cs from high activity waste simulant using resorcinol formaldehyde polycondensate resin: batch and column studies, *Sep. Sci. Technol.* 48 (2013) 133–139.
- [35] P. Loganathan, S. Vigneswaran, J. Kandasamy, N.S. Bolan, Removal and recovery of phosphate from water using sorption, *Crit. Rev. Environ. Sci. Tech.* 44 (2014) 847–907.
- [36] N. Moazezi, M.A. Moosavian, Removal of rubidium ions by polyaniline nanocomposites modified with cobalt-Prussian blue analogues, *J. Environ. Chem. Eng.* 4 (2016) 2440–2449.
- [37] B. Hashemi, M. Shamsipur, Synthesis of novel ion-imprinted polymeric nanoparticles based on dibenzo-21-crown-7 for the selective pre-concentration and recognition of rubidium ions, *J. Sep. Sci.* 38 (2015) 4248–4254.
- [38] P. Zhang, Y. Wang, D. Zhang, Removal of Nd (III), Sr (II), and Rb (I) ions from aqueous solution by thiacalixarene-functionalized graphene oxide composite as an adsorbent, *J. Chem. Eng. Data* 61 (2016) 3679–3691.
- [39] Z.H. Liu, K. Ooi, Preparation and alkali-metal ion extraction/insertion reactions with nanofibrous manganese oxide having 2×4 tunnel structure, *Chem. Mater.* 15 (2003) 3696–3703.
- [40] S. Taj, D. Muhammad, M.A. Chaudhry, M. Mazhar, Lithium, rubidium and cesium ion removal using potassium iron(III) hexacyanoferrate(II) supported on polymethylmethacrylate, *J. Radioanal. Nucl. Chem.* 288 (2011) 79–88.
- [41] X. Ye, Z. Wu, W. Li, H. Liu, Q. Li, B. Qing, M. Guo, F. Go, Rubidium and cesium ion adsorption by an ammonium molybdophosphate-calcium alginate composite adsorbent, *Colloids Surf. A* 342 (2009) 76–83.
- [42] D.L. Guerra, A.C. Batista, R.R. Viana, C. Airoidi, Adsorption of rubidium on raw and MTZ- and MBI-imogolite hybrid surfaces: An evidence of the chelate effect, *Desalination* 275 (2011) 107–117
- [43] Y. Fang, H. Zhao, W. Dai, L. Ma, N. Ma, Enhanced adsorption of rubidium ion by a phenol@MIL-101 (Cr) composite material, *Microporous and Mesoporous Mater.* 251 (2017) 51–57

- [44] P.V. Medeiros, F. de Brito Mota, A.J. Mascarenhas, C.M. de Castilho, Adsorption of monovalent metal atoms on graphene: a theoretical approach, *Nanotechnology*, 21 (2010) 115701.
- [45] E. Güler, E., C. Kaya, N. Kabay, M. Arda, Boron removal from seawater: State-of-the-art review, *Desalination* 356 (2015) 85–93.
- [46] ANZECC and ARMCANZ, Australian and New Zealand guidelines for fresh and marine water quality, Australian and New Zealand Environment and Conservation Council and Agriculture and Resource Management Council of Australia and New Zealand, Canberra, 2000, pp. 1-103.
- [47] R. Chakravarty, R. Ram, K.T. Pillai, Y. Pamale, R.V. Kamat, A. Dash, Ammonium molybdophosphate impregnated alumina microspheres as a new generation sorbent for chromatographic $^{137}\text{Cs}/^{137\text{m}}\text{Ba}$ generator, *J. Chromatogr. A* 1220 (2012) 82–91.

Supplementary data for

**Rubidium removal by membrane adsorption hybrid system using
potassium cobalt hexacyanoferrate**

T. Nur, P. Loganathan, M.A.H. Johir, J. Kandasamy, S. Vigneswaran

*Faculty of Engineering, University of Technology Sydney (UTS), P.O. Box 123, Broadway, NSW 2007,
Australia*

**Corresponding author. Tel.: +61 2 95142641, fax: +61 2 95142633.*

Email: s.vigneswaran@uts.edu.au

Table S1.

The adsorption capacity of KCoFC and AMP in MAHS experiments.

Adsorbent	Particle size (mm)	Solution type	Dose (g/L)	Total amount of adsorbent added (g)	Flux (L/m ² h)	Adsorption capacity (mg/g)
KCoFC	< 0.075	Rb 5 mg/L	0.05	1.5	10	62
			0.10	2.9	10	42
			0.10	2.9	20	69
			0.20	5.8	10	24
		Synthetic seawater	0.20	5.8	10	16
AMP	< 0.075	Rb 5 mg/L	0.20	5.8	10	14

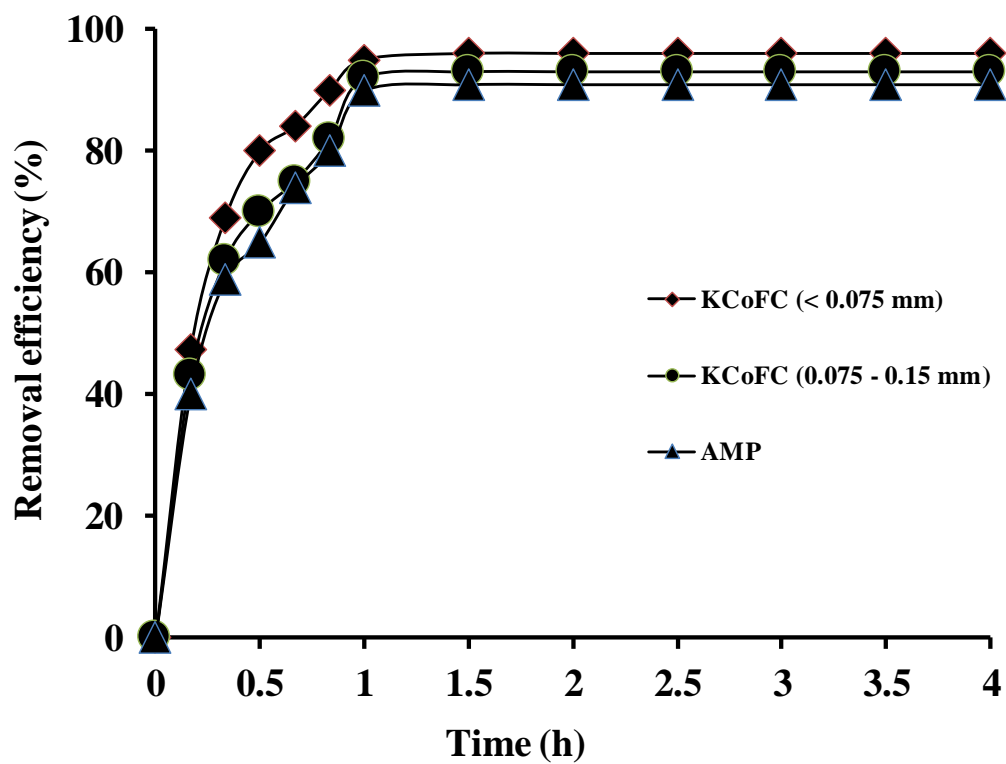


Fig. S1. Effect of time on Rb removals by KCoFC and AMP.

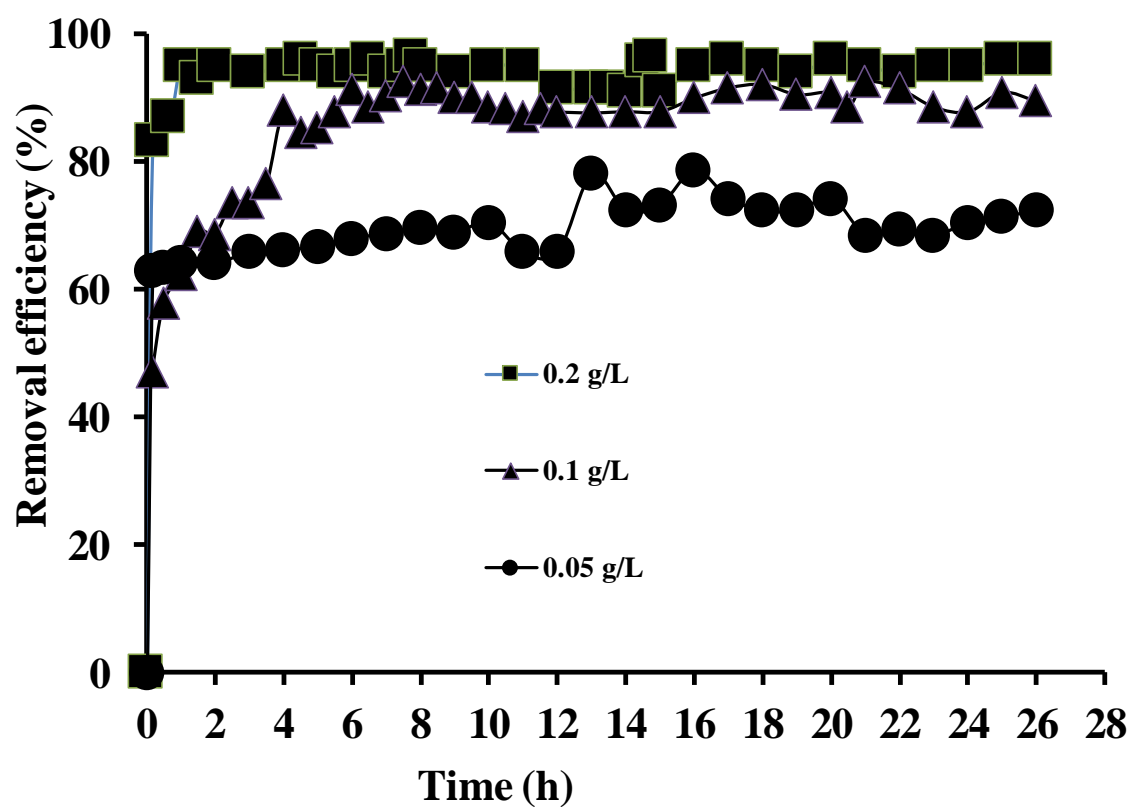


Fig. S2. Effect of initial KCoFC doses with repeated additions of 25% of the doses every hour on Rb removal efficiency in MAHS (influent concentration of Rb 5 mg/L; flux 10 L/ m²h).

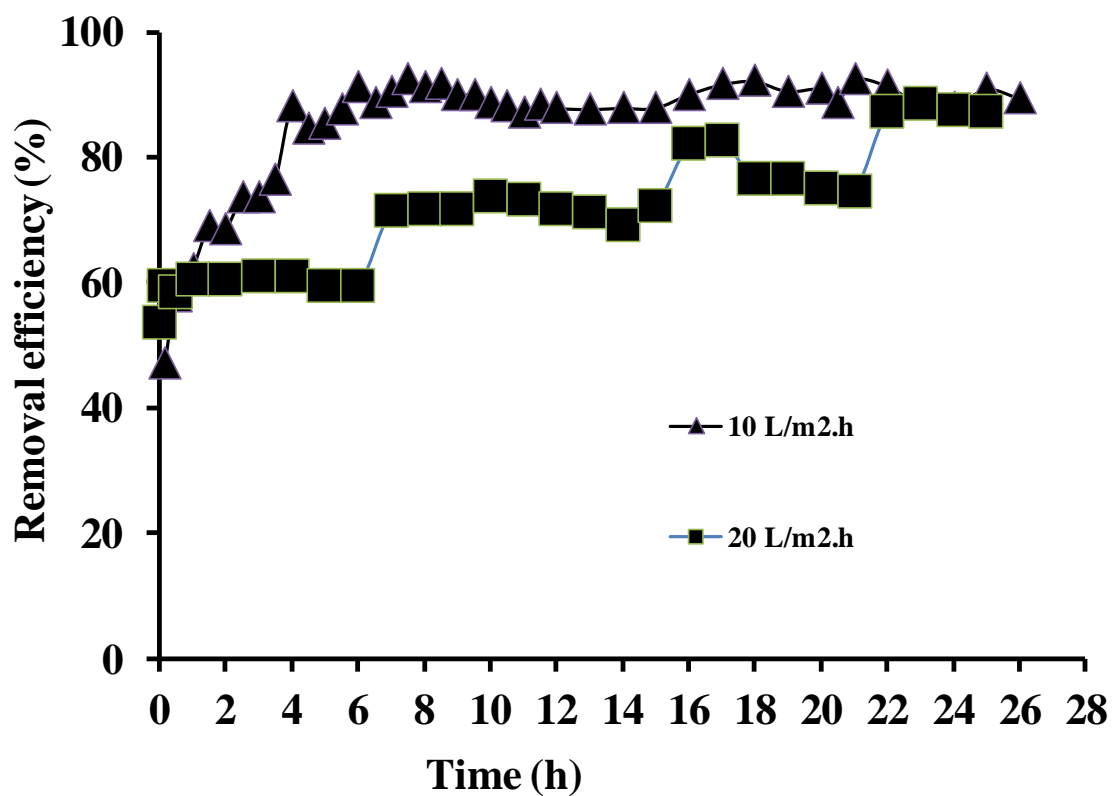


Fig. S3. Effect of flux on Rb removal efficiency by KCoFC with repeated additions of 25% of the initial dose every hour in MAHS (inlet concentration of Rb 5 mg/L; initial adsorbent dose 0.1 g/L of membrane reactor volume).

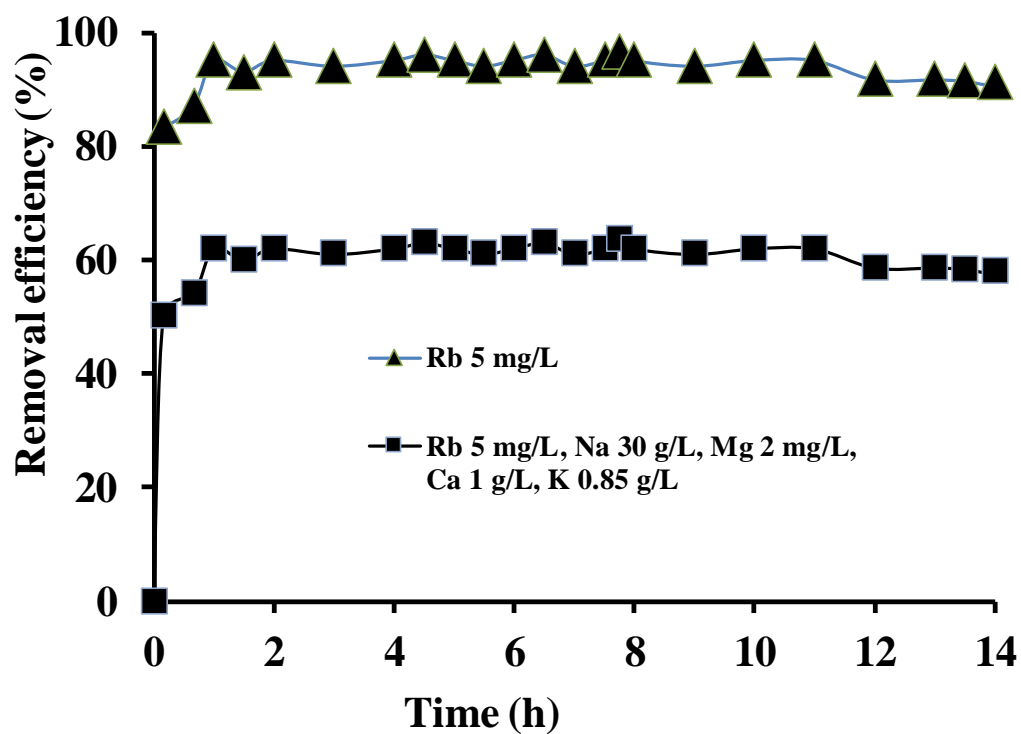


Fig. S4. Effect of seawater co-ions on Rb removal efficiency by KCoFC with repeated additions of 25% of the initial dose every hour in MAHS (flux 10 L/ m²h; initial adsorbent dose 0.2 g/L of membrane reactor volume).

ACCEPTED MANUSCRIPT

Research Highlights

- KCoFC efficiently removed Rb in the membrane adsorption hybrid system (MAHS).
- Maximum Rb adsorption capacity of finer-sized KCoFC in MAHS was 69 mg/g.
- Rb removal decreased by only 33% in seawater with elevated levels of other ions.
- Sequence of KCl desorption, resin adsorption, HCl desorption produced pure Rb.

ACCEPTED MANUSCRIPT